

## Accepted Manuscript

EPR, DFT and Electrochemical Interpretation of a Cu(II) Derivative Incorporating a Schiff Base Precursor

Kuheli Das, Sanchita Goswami, Belete B. Beyene, Amogne W. Yibeltal, Eugenio Garribba, Antonio Frontera, Amitabha Datta

PII: S0277-5387(18)30783-6  
DOI: <https://doi.org/10.1016/j.poly.2018.11.058>  
Reference: POLY 13605

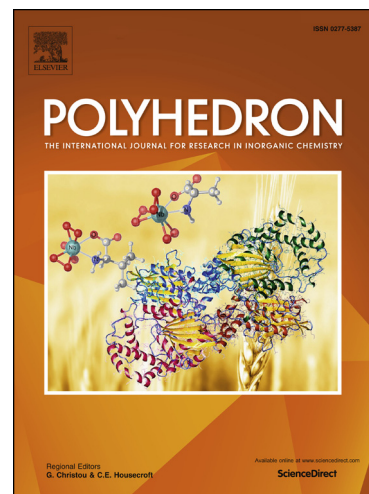
To appear in: *Polyhedron*

Received Date: 13 November 2018

Accepted Date: 26 November 2018

Please cite this article as: K. Das, S. Goswami, B.B. Beyene, A.W. Yibeltal, E. Garribba, A. Frontera, A. Datta, EPR, DFT and Electrochemical Interpretation of a Cu(II) Derivative Incorporating a Schiff Base Precursor, *Polyhedron* (2018), doi: <https://doi.org/10.1016/j.poly.2018.11.058>

This is a PDF file of an unedited manuscript that has been accepted for publication. As a service to our customers we are providing this early version of the manuscript. The manuscript will undergo copyediting, typesetting, and review of the resulting proof before it is published in its final form. Please note that during the production process errors may be discovered which could affect the content, and all legal disclaimers that apply to the journal pertain.



# EPR, DFT and Electrochemical Interpretation of a Cu(II) Derivative Incorporating a Schiff Base Precursor

Kuheli Das,<sup>\*a</sup> Sanchita Goswami,<sup>a</sup> Belete B. Beyene,<sup>b,d</sup> Amogne W. Yibeltal,<sup>b,c</sup>

Eugenio Garribba,<sup>e</sup> Antonio Frontera,<sup>f</sup> Amitabha Datta,<sup>\*b</sup>

<sup>a</sup> Department of Chemistry, University of Calcutta, 92 A.P.C. Road, Kolkata -  
700009, India

<sup>b</sup> Institute of Chemistry, Academia Sinica, Nankang, Taipei – 115, Taiwan

<sup>c</sup> Department of Applied Chemistry, National Chiao-Tung University, Hsinchu – 300,  
Taiwan

<sup>d</sup> Department of Chemistry, Bahir Dar University, P.O. Box – 79, Bahir Dar, Ethiopia

<sup>e</sup> Dipartimento di Chimica e Farmacia, Università di Sassari, Via Vienna 2, I-07100  
Sassari, Italy

<sup>f</sup> Departament de Química, Universitat de les Illes Balears, Crta de Valldemossa km  
7.5, 07122 Palma de Mallorca (Balears), Spain

\*Corresponding authors. [kuheli.chemistry@gmail.com](mailto:kuheli.chemistry@gmail.com) (K. Das),

[amitd\\_ju@yahoo.co.in](mailto:amitd_ju@yahoo.co.in) (A. Datta)

## Abstract

The mononuclear Cu<sup>II</sup> derivative, [Cu(L)(H<sub>2</sub>O)<sub>2</sub>] (**1**) [where H<sub>2</sub>L = *N,N'*-bis(3-methoxysalicylideneimino)-1,3-diaminopropane] is afforded and systematically characterized. In **1**, the central Cu<sup>II</sup> atom is linked to the NNOO donor atoms of the di-compartmental Schiff base precursor and additionally coordinated with two water molecules; thus achieves a distorted octahedral geometry. The EPR spectrum is simulated with WinEPR software having  $g_{\parallel} = 2.210$  and  $g_{\perp} = 2.041$ . We also conduct the DFT computational study which fits well with experimental affirmation. The room temperature magnetic susceptibility of complex **1** confirms the effective magnetic moment ( $\mu_{\text{eff}}$ ) value as 1.99 B.M. The electrochemical measurement using cyclic voltammetry showed redox potentials at +0.63, -1.25, and -1.82 V vs Ag/AgCl, which are due to reversible and rapid Cu(III/II), Cu(II/I) and Cu(I/0) process.

---

*Keywords:* Cu(II); Crystal structure; EPR; DFT; Redox

## 1. Introduction

Metal complexes incorporating different N,O donor ligands have received considerable attention due to their ability to bind different cations [1], anions [2,3], and neutral compounds [4,5]. The choice of ligands encoding some degree of flexibility is an important factor in the design of metal-ligand complexes of different nuclearity, dimensionality, redox ability, chirality, etc. which illustrates a range of applications in selective host-guest recognition [6-9]. The coordination behaviour of Schiff bases [10-15] has been drawing an immense interest since long back because of their preparative accessibilities, structural variety, varied denticity and subtle steric and/or electronic control on their frameworks leading to the formation of complexes of not only different coordination numbers but also of different nuclearities those possess interesting molecular and crystalline architectures [16-19] and related properties [20,21]. Tetradentate Schiff bases with N<sub>2</sub>O<sub>2</sub> donor set atoms provide suitable coordination environments with metal ions; thus can readily form a wide variety of metal derivatives complexes with copper(II) ions [22,23]. The hexacoordinated Cu(II) ion with d<sup>9</sup> configuration prefers distorted octahedral geometry which is a direct consequence of Jahn–Teller effect [24]. Thus, with a set of four strongly and two weakly coordinating ligands, the later two always occupy the axial positions. The distortion is usually seen as axial elongation, consistent with the lability and geometric flexibility of the complex. The combined application of

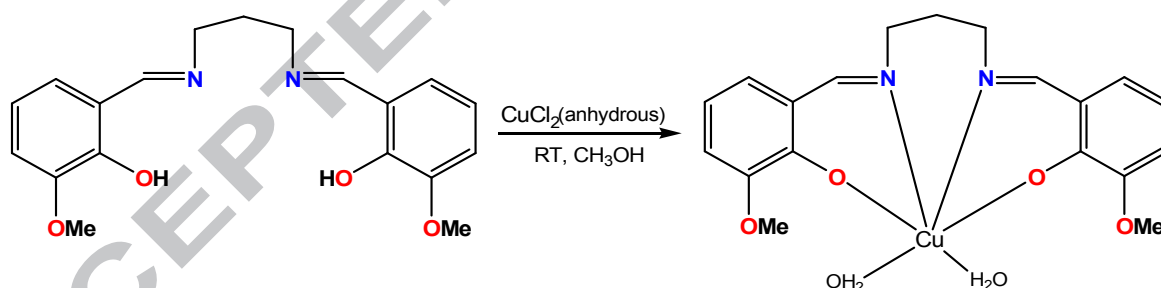
theoretical methods and experimental techniques has highly interest for many years to determine the structural and spectroscopic properties of compounds. Over the past ten years, the computational methods based on DFT were found the favorite ones, and much information can be obtained on the molecular geometry, vibrational frequencies, atomic charges etc. [25,26].

Before some of us have reported few metal complexes incorporating tetradentate Schiff base ligands [27-29]. Here, we utilize the potentially di-compartmental hexadentate Schiff base precursor [30], *N,N'*-bis(3-methoxysalicylideneimino)-1,3-diaminopropane ( $H_2L$ ) to afford the Cu(II) derivative,  $[Cu(L)(H_2O)_2]$  (**1**). This Schiff baseligand has both the internal  $N_2O_2$  cavity and the external  $O_2O_2$  cavity. To utilize only the internal  $N_2O_2$  cavity, we accommodate one 3d metal ion, Cu(II) and to fulfill the octahedral geometry of the metal ion, two water molecules are coordinated from axial positions. Besides the structural elucidation, we report the EPR spectra, DFT computation and electrochemical study of the Cu(II) derivative.

## 2. Results & discussion

### 2.1. Synthesis and characterization

The Schiff base precursor, H<sub>2</sub>L [where H<sub>2</sub>L = *N,N'*-bis(3-methoxysalicylideneimino)-1,3-diaminopropane] is acquired from the condensation of *o*-vanillin and 1,3-diaminopropane [30]. The stoichiometric reaction of H<sub>2</sub>L and anhydrous CuCl<sub>2</sub> in methanol affords compound **1** in moderate yield (see Scheme 1). The infrared spectrum (KBr pellet, 400 – 4000 cm<sup>-1</sup>) of compound **1** is consistent with the structural data given in this paper. A weak broad band in the region 3600-3400 cm<sup>-1</sup> due to hydrogen bonds involving the OH group in free Schiff base is absent in the metal derivative. This indicates that the phenolic oxygen is deprotonated and coordinated with Cu(II) [31]. The strong ν<sub>C=N</sub> band appeared at 1634 cm<sup>-1</sup> in **1**, indicates that the azomethine nitrogen atom is coordinated with Cu(II) [32-34].



**Scheme 1.** Formation of compound **1**.

Sharp bands appearing at nearly 496 and 421 cm<sup>-1</sup> correspond to the Cu–N and Cu–O stretching frequencies, respectively. In compound **1**, a band at 358 nm may be assigned to the n→π\* transition of the imine group [35] and the band at higher energy (269 nm) is associated with the aromatic π→π\* intra-ligand charge-transfer transition. A broad band in the range 620– 650 nm can be correlated to a d-d transition, which is

typical for a Cu(II) Schiff base complex [36]. The X-ray diffraction analysis confirms that the resulting compound **1** is a mononuclear octahedral Cu(II) derivative.

## 2.2. Crystal structure

Single-crystal X-ray diffraction analysis reveals that compound **1** crystallizes in the orthorhombic system having space group *Pnma*. The molecular structure of compound **1** is depicted in **Figure 1**; selected bond distances and angles are listed in **Table 1**. The title compound attributes a six-coordinated Cu(II) center with the internal N<sub>2</sub>O<sub>2</sub> cavity of the hexa-dentate Schiff base ligand and two coordinated water molecules. The pair of N<sub>imine</sub> atoms (N1 and N1') and O<sub>phenolic</sub> atoms (O1 and o1') of the Schiff base ligand define the equatorial plane. Two O<sub>water</sub> molecules (O3 and O4) belong at the axial position at distances, 2.089(2) and 2.103 (2) Å, respectively. The bond angles around the Cu(II) ion are slightly distorted from those of a regular octahedron and range from 86.03(6)° to 175.40(9)°. The two O<sub>water</sub> molecules lie at the *trans* position of the octahedron. The *cis* Ni-O<sub>phenolic</sub> bond lengths [2.015(2) Å] is considerably smaller than the *trans* Ni-O<sub>water</sub> bond lengths [2.089(2) and 2.103(2) Å] (**Table 1**). Deviation of atoms from the least-squares plane formed by O(1), N(1), O(1'), and N(1') is 0.22-0.24 Å. Thus the angles, O(1)-Cu(1)-N(1) and N(1)-Cu(1)-N(1') are either lesser or greater than the ideal value of 90°. The *trans* angles O(1)-

Cu(1)-N(1) and N(1')-Cu(1)-O(1') deviate from the ideal bond angle of 180°. The N(1)-Cu(1)-N(1') angle is 97.10(7)° and is typical of six-membered chelate ring [37-40]. The two six-membered chelate-rings defined by the metal and corresponding *o*-vanillin and amine moiety are not planar; deviated....The phenyl ring of the ligand lies approximately on the same plane of the three chelate cycles. This is probably a result of some conjugation between the aromatic system of phenyl group and pseudoaromatic system of the six-membered chelate ring.

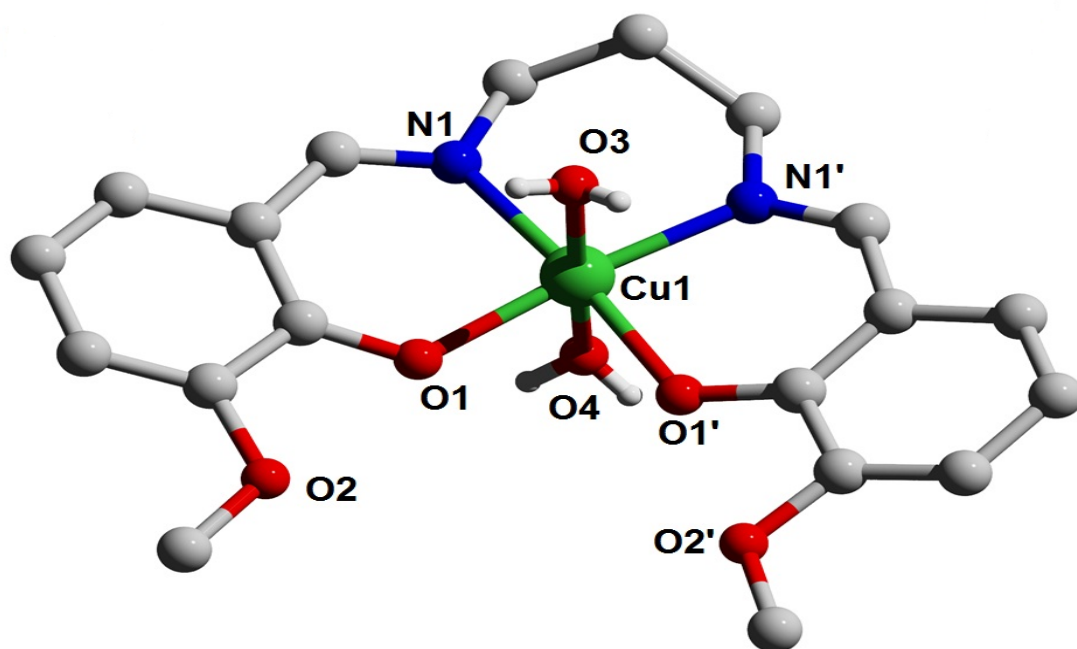


**Figure 1.** The molecular structure of complex **1**. The hydrogen atoms are not mentioned for clarity.

### 2.3. EPR spectra

EPR spectra were recorded on the polycrystalline powder of complex **1** at 298 and 100 K (**Figure 2**). As it is possible to note the resolution improves significantly with

lowering the temperature. At 298 K the dipolar interaction and intercenter exchange between neighbouring units broaden the hyperfine lines, [41] and only one isotropic absorption centred at  $g = 2.010$  is revealed (**Figure 2a**). At 100 K, the spectrum becomes axial with two transitions centred in the range 304-305 mT and around 330 mT were observed (**Figure 2b**). The spectrum was simulated with WinEPR software with  $g_{\parallel} = 2.210$  and  $g_{\perp} = 2.041$  (**Figure 2c**). The order  $g_{\parallel} \gg g_{\perp} > g_e$  indicates a ground state based on the Cu orbital  $d_{x^2-y^2}$  and support the elongated octahedral geometry determined by X-ray diffraction analysis [42-44]. Complex **1** was dissolved in DMF, DMSO and CH<sub>3</sub>OH to examine the behavior in solution (**Figure 3**). In all the three cases mononuclear Cu(II) species were detected with the spin Hamiltonian parameters listed in **Table 2**. The values of  $g_z$  are in the range 2.242-2.244, while those of  $A_z$  in the range  $186-187 \times 10^{-4} \text{ cm}^{-1}$ , with the rhombicity of  $x$  and  $y$  axes being small. These parameters are characteristic of the Cu(II)-salpn complexes, where salpn indicates *N,N'*-propylenediamine-bis(salicylideneimine) anion; the coordination mode is (O<sup>-</sup>, N, N, O<sup>-</sup>). The experimental parameters measured are similar to those measured for similar ligands [45-50,27]. In DMSO and DMF it is

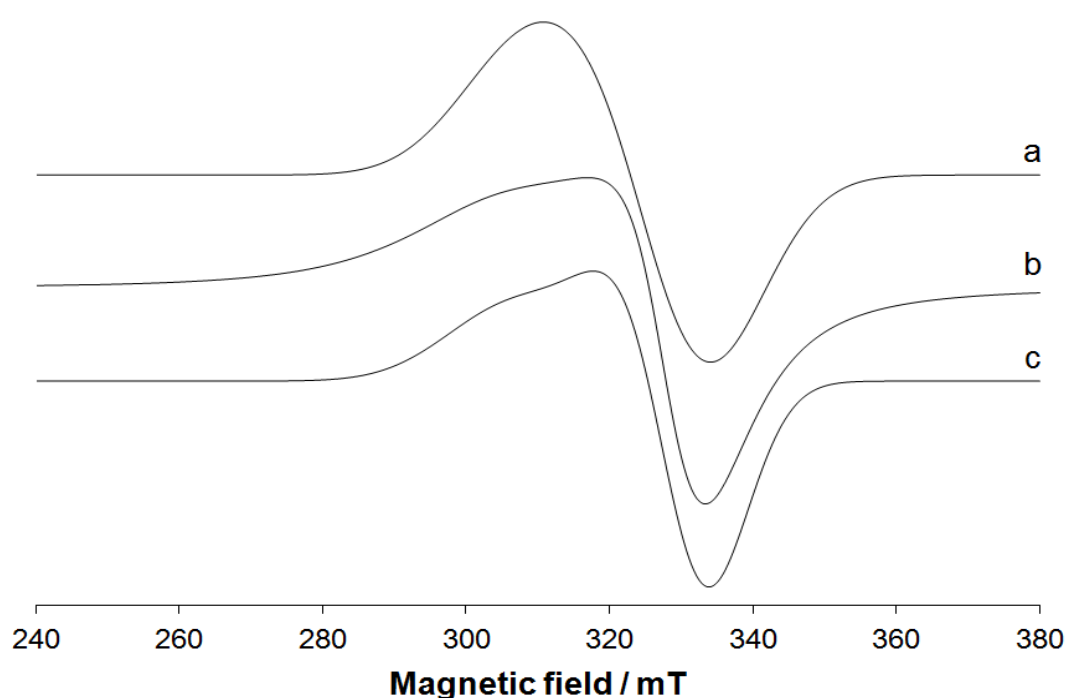


**Figure 2.** X-band EPR spectra recorded at 77 K on the polycrystalline powder of complex **1**: (a) 298 K and (b) 100 K. In the trace c the simulation of the spectrum at 100 K is also reported.

possible to observe, even if not perfectly resolved, the superhyperfine coupling between the unpaired electron on copper with the two  $^{14}\text{N}$  nuclei of the ligand. If the spin Hamiltonian parameters are compared with those of the analogous species formed by salen, *N,N'*-ethylenediamine-bis(salicylideneimine), a decrease of  $A_z$  can be noticed (the hyperfine coupling constants along the  $z$  axis for  $[\text{Cu}(\text{salen})]$  is reported in the range  $194\text{-}209 \times 10^{-4} \text{ cm}^{-1}$ ) [51-55]. The reason can be assigned to the weak axial coordination of solvent – as in the solid state – to give species with

composition  $[\text{Cu}(\text{salpn})(\text{Solvent})_2]$  or – alternatively – to the different chelate ring formation ((6,6,6) rings for salpn ligands and (6,5,6) for salen derivatives).

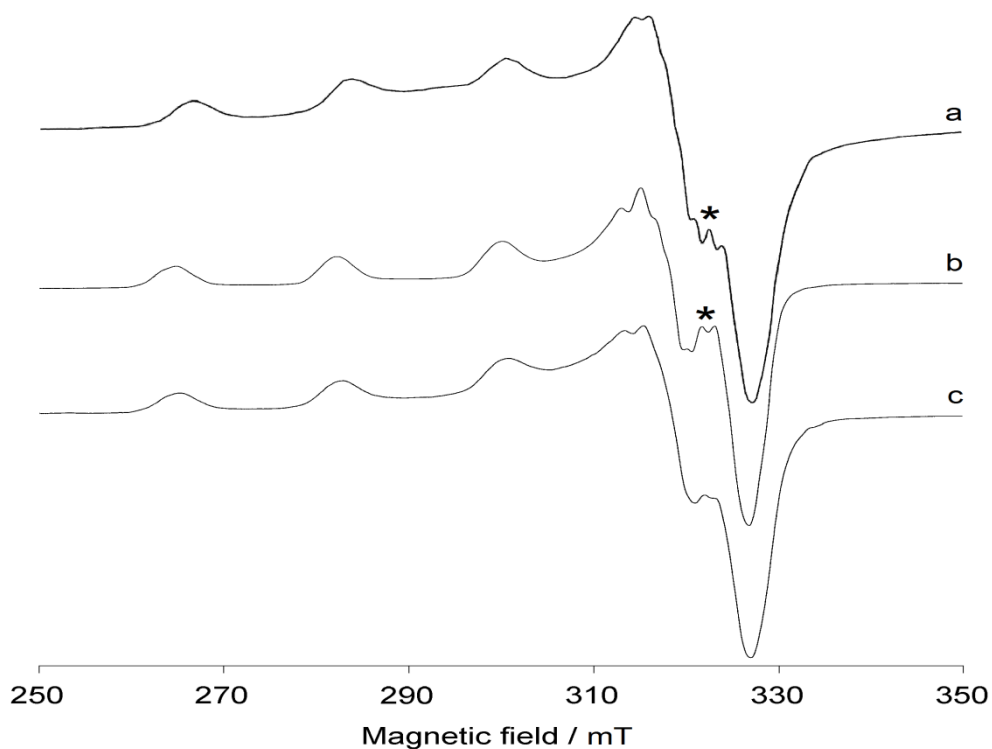


**Figure 3.** Anisotropic X-band EPR spectra recorded at 100 K on the polycrystalline powder of complex **1** dissolved in: (a) DMSO; (b) DMF and (c)  $\text{CH}_3\text{OH}$ . With the asterisks the resonances due to the superhyperfine coupling between the unpaired electron on copper with the two nuclei of  $^{14}\text{N}$  nuclei is shown.

**Table 2.** Spin Hamiltonian EPR parameters of complex **1** in organic solution.<sup>a</sup>

Solvent	$g_x$	$g_y$	$g_z$	$A_x$	$A_y$	$A_z$
DMSO	2.036	2.068	2.243	11	13	187
DMF	2.036	2.069	2.244	11	13	187
$\text{CH}_3\text{OH}$	2.037	2.068	2.242	12	13	186

<sup>a</sup>  $A$  values reported in  $10^{-4} \text{ cm}^{-1}$ .

#### 2.4. DFT computation

The calculated values of the g-tensor components at the B3LYP/def2-TZVP level of theory for the X-ray structure of **1** are  $g_z = 2.289$ ,  $g_x = 2.087$ ,  $g_y = 2.098$ , which correlate well with the experimental values and indicate a ground state based on the Cu- $d_{x^2-y^2}$  orbital for which  $g_z > g_x \sim g_y$  is expected. Indeed, the SOMO and spin density plots shown in **Figure 4** confirm the presence of the unpaired electron in the  $d_{x^2-y^2}$  orbital.

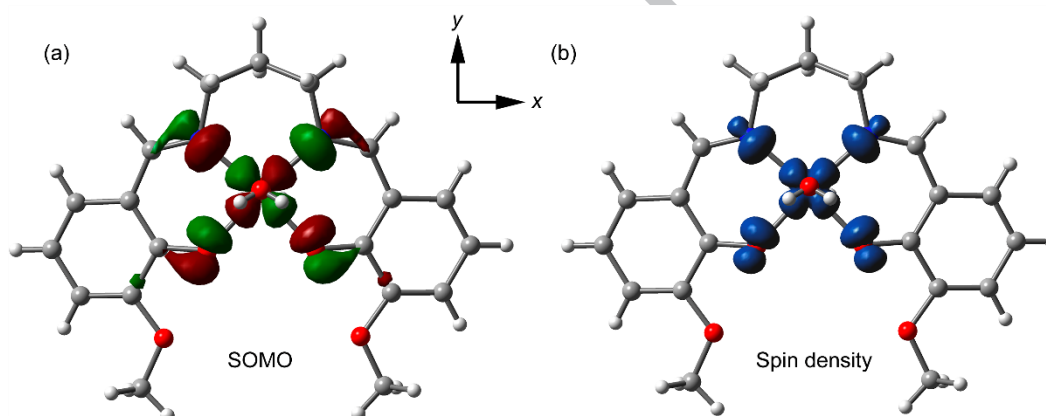


**Figure 4.** SOMO (a) and spin density plot (b) of the X-ray of **1**. At the B3LYP/def2-TZVP level of theory.

We have also carried out DFT calculation using the [Cu(salpn)] ( $S = \frac{1}{2}$ ) complex in solution, without the water molecules in apical positions. Since in the three solvents (DMSO, DMF and MeOH) the EPR experiment gives almost identical results, we have used only DMF to analyze the square planar complex. The spin Hamiltonian

parameters  $g_z$  and  $A_z$  are 2.24 and  $172.5 \times 10^{-4} \text{cm}^{-1}$ , respectively, which are also in good agreement with the experimental results gathered in **Table 2**. In case of the inclusion of weakly coordinated solvent molecules in the apical positions, the values slightly change to  $g_z = 2.28$  and  $A_z = 177.6 \times 10^{-4} \text{cm}^{-1}$ , the latter is closer to the experimental data, thus suggesting the presence of solvent molecules above and below the  $\text{CuO}_2\text{N}_2$  moiety.

### 2.5. Room temperature magnetic susceptibility study

The Cu(II) complexes usually have distorted octahedral geometry, but many complexes of square-planar or approximately tetrahedral geometry are also known [56]. However, stereochemistry has little effect on the magnetic moments of Cu(II) complexes and values slightly above the spin-only value for one unpaired electron, are expected [56]. A regular octahedral Cu(II) complex has the ground term  ${}^2E_g$  and hence there is probability of no orbital contribution. The spin-only value corresponding to one unpaired electron is 1.73 B.M., but the observed values belong usually in the range 1.80-2.10 BM. The slightly higher value is due to the spin-orbit coupling [56]. Complex **1** shows room temperature magnetic susceptibility value as expected for an isolated  $d^9$  transition metal center. The effective magnetic moment

( $\mu_{\text{eff}}$ ) value is found to be 1.99 B.M. at 300 K, which is very consistent with expected spin-only magnetic moment of a  $S = 1/2$ ,  $d^9$  copper (II) system.

## 2.6. Electrochemical study

The electrochemical measurement was carried using cyclic voltammetry technique. The voltammogram of 1 mM of complex **1** in DMSO using 0.1 M  $[\text{Bu}_4\text{N}[\text{PF}_6]]$  as supporting electrolyte, glassy carbon as working, Pt wire as counter and silver as reference electrode at room temperature is shown in **Figure 5**. The solution purged with  $\text{N}_2$  gas for 5 minutes prior to CV measurement in order to avoid the residue peak due to dissolved oxygen. Up on oxidative scanning from 0 to +1.0 and reductive scanning from 0 to -2.1 V vs Ag/AgCl, three reversible peaks were observed at  $E_{1/2} = +0.63$ , -1.25 and -1.82 V vs Ag/AgCl. The starting complex is Cu(II) and under electrochemical condition, electron transfer occur between complex solution and electrode. We presumed that the electrochemical redox behavior of the complex is due to redox active central metal (copper) in the complex, as the ligand is electrochemically silent in the potential window where the complex shows redox potentials. Hence the reversible redox potential at  $E_{1/2} = +0.63$  V vs Ag/AgCl (**Figure 5a**) is assigned to Cu(II/III) redox couple, while the redox potential peak at  $E_{1/2} = -1.25$  vs Ag/AgCl is due to Cu(II/I). The weak reversible redox potential peak at -1.82

V vs Ag/AgCl could be assigned to Cu(I/0) redox event (**Figure 5b**).

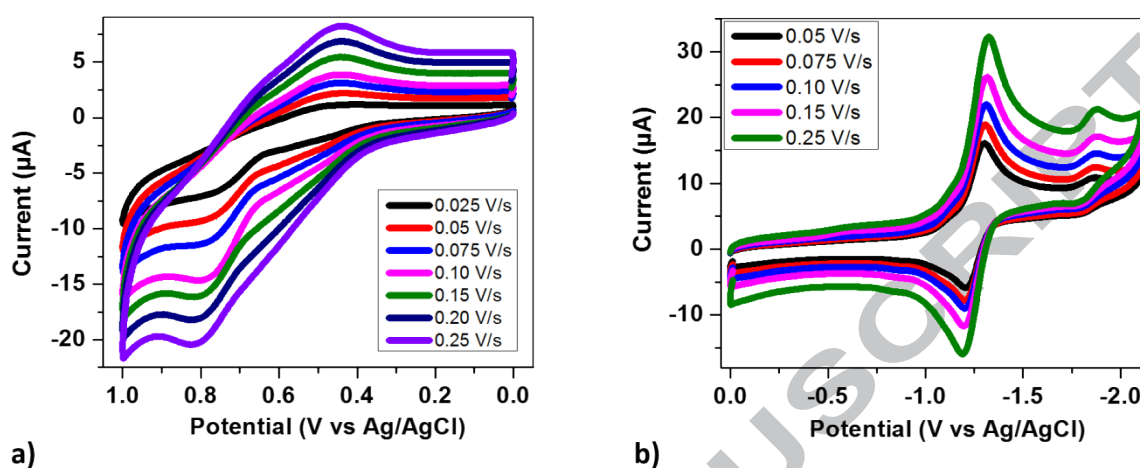


**Figure 5.** Cyclic voltammogram of 1 mM of complex **1** in dry DMSO solution containing 0.1 M  $[\text{Bu}_4\text{N}]\text{PF}_6$  using glassy carbon as working electrode, Pt wire as counter and silver as reference electrode at room temperature; a) oxidative scan b) reductive scan.

The scan rate dependent study showed that both the cathodic and anodic peaks of the complex increase when the scan rate is increased (**Figure 6**). At a slow scan rate, the diffusion layer grows much further from the electrode in comparison to a fast scan. Consequently, the flux to the electrode surface (which is directly proportional to the current) is considerably smaller at slow scan rates than it is at faster scan rates. Hence, the cathodic or anodic current is lower at slow scan rates and higher at high rates

[57,58].

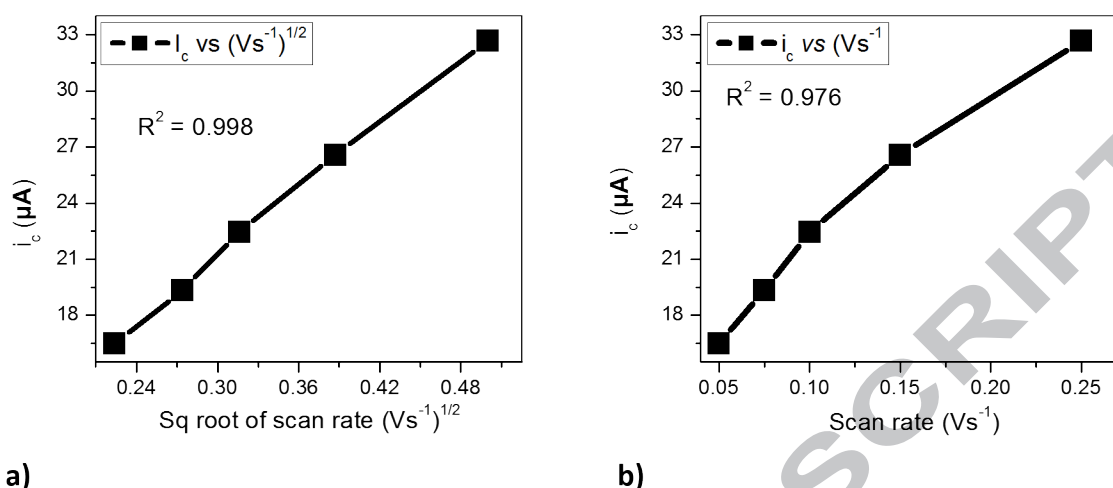


**Figure 6.** Linear fit of: (a) Square root of the scan rate vs cathodic peak current and (b) the scan rate vs cathodic peak current.

Moreover, the scan rate study shows that the potential of current maximum peak does not alter at different scan rates and this is a characteristic of electrode reaction, which has rapid electron transfer kinetics, and is reversible. The information gathered from scan rate dependent study is also important to predict whether the electrochemical process is surface controlled (adsorption controlled) or diffusion controlled. For this analysis, we choose the cathodic peak current at  $-1.25$  V vs Ag/AgCl. As can be seen from **Figure 6**, the magnitude of cathodic peak current ( $i_c$ ) is directly proportional to square root of scan rate (**Figure 6a**) and the scan rate (**Figure 6b**). This strongly suggest that the electrochemical process involving Cu(II/I) of the complex is a mixture of diffusion controlled and adsorption (surface) controlled process [57].

However, the better linear relationship of cathodic current peak with square root of scan rate shows that the electrochemical process is predominantly a diffusion-controlled process. It means that the electroactive species is part of a solution (not confined to the electrode surface) and the redox process depends on the rate at which the molecule diffuse from the solution to electrode surface.

### 3. Conclusion

The mononuclear Cu<sup>II</sup> derivative is afforded incorporating the hexadentate Schiff base precursor, [2-((E)-(2-(2-aminoethylamino)ethylimino)methyl)-6-methoxyphenol] (H<sub>2</sub>L). The solid state structure of **1** shows that the central Cu<sup>II</sup> atom possesses on an octahedral environment. The compound is systematically characterized by IR and UV-vis spectral techniques; EPR spectroscopy in different solvents (CH<sub>3</sub>OH, DMSO and DMF) is measured and the values of  $g_z$  are in the range 2.242-2.244, while those of  $A_z$  in the range  $186-187 \times 10^{-4} \text{ cm}^{-1}$ . DFT computation is governed to confirm the geometry as well as the spectral evidence. On electrochemical study, compound **1** shows three reversible redox potentials when the CV scanned from +1.0 to -2.1 V vs Ag/AgCl, owing to copper based redox events with performance of diffusion controlled process. Further exploration on anti-mycobacterial, DNA binding and cell-imaging studies subjecting this compound currently is in progress.

## Acknowledgments

KD expresses her appreciation to the SERB (Science and Engineering Research Board, India) Grant (PDF/2016/002832) for financial assistance.

## Statement

We wish to assure that our manuscript does not contain any potential interest or "no conflict of interest".

## 4. Experimental Section

### 4.1. Materials

All the experiments were carried out under aerobic conditions.  $\text{Cu}(\text{ClO}_4)_2 \cdot 6\text{H}_2\text{O}$  was purchased from Aldrich Chemicals. 1,3-diaminopropane and *o*-vanillin were purchased from Merck, India. Solvents were of reagent grade and used without further purification.

*Caution!* Perchlorate salts in presence of organic materials are potentially explosive.

They should be prepared in small amounts and handled with extreme care.

### 4.2. Physical measurements

Microanalytical data (C, H, and N) were collected on a Perkin–Elmer 2400 CHNS/O

elemental analyzer. FTIR spectra were recorded on a Perkin-Elmer RX-1 spectrophotometer in the range 4000–400  $\text{cm}^{-1}$  as KBr pellets. Electronic spectra were measured on a Perkin-Elmer Lambda 25 (U.V.–Vis.–N.I.R.) spectrophotometer. EPR spectra were recorded from 0 to 8000 Gauss at liquid nitrogen temperature (100 K) or room temperature (298 K) with an X-band Bruker EMX spectrometer equipped with a HP 53150A microwave frequency counter. The microwave frequency was in the range 9.40-9.41 GHz, microwave power was 20 mW (which is, with the ER4119 HS resonator, below the saturation limit), time constant was 81.92 ms, modulation frequency 100 kHz, modulation amplitude 0.4 mT, resolution 4096 points. EPR spectrum of **1** solid at LT (**Figure 2**) was simulated with WinEPR SimFonia software [59], with linewidths of 13, 13 and 18 mT for the *x*, *y* and *z* directions and a ratio Lorentzian/Gaussian of 1. The cyclic voltammetry measurements were carried out on CHI 621B electrochemical analyzer (CH Instruments, Austin, TX, USA) in DMSO containing 0.1 M tetra *n*-butylammonium hexafluorophosphate [ $\text{Bu}_4\text{N}(\text{PF}_6)$ ] as the supporting electrolyte. The cell assembly consists of a glassy carbon as the working electrode, Ag/AgCl as reference electrode, and Pt wire as the counter electrode.

Synthesis of  
Bis(3,5-di-tert-  
butylpyrazol-1-  
yl)methane  
(bdtbpzm) (2):  
3,5-Di-tert-  
butylpyrazole (3.00  
g, 16.64 mmol),  
KOH (3.60 g,

64.16 mmol), K

2

CO

3

(9.00 g, 65.12

mmol) and

benzyltriethylam-

monium chloride

(0.5 g) were

dissolved in  
dichloromethane  
(100 mL) and  
heated under reflux  
for 5 hours. Salts  
were removed  
by filtration and the  
filtrate was

concentrated in  
vacuo to dryness.

The white residue  
was dissolved in  
water and extracted  
with pent-  
ane (2 3 150 mL).

The organic layer  
was dried (MgSO

) and the solvent removed in vacuo. The white residue was recrystallized from pentane to give bdtbpzm (2) as a white powder, which was

dried in vacuo.

Yield 2.40 g (77%)

Synthesis of

Bis(3,5-di-tert-

butylpyrazol-1-

yl)methane

(bdtbpzm) (2):

3,5-Di-tert-

butylpyrazole (3.00

g, 16.64 mmol),

KOH (3.60 g,

64.16 mmol), K

<sub>2</sub>

CO

<sub>3</sub>

(9.00 g, 65.12

mmol) and

benzyltriethylam-

monium chloride  
(0.5 g) were  
dissolved in  
dichloromethane  
(100 mL) and  
heated under reflux  
for 5 hours. Salts  
were removed

by filtration and the  
filtrate was

concentrated in  
vacuo to dryness.

The white residue  
was dissolved in  
water and extracted

with pent-

ane (2 3 150 mL).

The organic layer

was dried (MgSO

4

) and the

solvent removed in

vacuo. The white

residue was

recrystallized

from pentane to give bdtbpzm (2) as a white powder, which was dried in vacuo.

Yield 2.40 g (77%)

Synthesis of

▶ Bis(3,5-di-tert-butylpyrazol-1-

yl)methane

(bdtbpzm) (2):

3,5-Di-tert-

butylpyrazole (3.00

g, 16.64 mmol),

KOH (3.60 g,

64.16 mmol), K

2

CO

3

(9.00 g, 65.12

mmol) and

benzyltriethylam-

monium chloride

(0.5 g) were

dissolved in

dichloromethane

(100 mL) and

heated under reflux

for 5 hours. Salts  
were removed  
by filtration and the  
filtrate was  
concentrated in  
vacuo to dryness.  
The white residue  
was dissolved in

water and extracted  
with pent-

ane (2 3 150 mL).

The organic layer  
was dried (MgSO

4

) and the

solvent removed in

vacuo. The white

residue was  
recrystallized  
from pentane to  
give bdtbpzm (2) as  
a white powder,  
which was  
dried in vacuo.

Yield 2.40 g (77%)

#### 4.3. Synthesis of the ligand ( $H_2L$ )

The Schiff base ligand, (*N,N'*-bis(3-methoxysalicylideneimino)-1,3-diaminopropane) is

synthesized by mixing o-vanillin (20 mmol, 3.04 g) with 1,3-diaminopropane (10 mmol, 0.833 ml) in 50 mL of MeOH. The orange solution is refluxed for 1 h, and after cooling down, the solvent is removed under reduced pressure to afford a deep-yellow crystalline solid which was collected as the ligand. Yield: 77%. Anal. Calc. for  $C_{19}H_{22}N_2O_4$ : C, 66.65; H, 6.48; N, 8.18. Found: C, 66.71; H, 6.42; N, 8.08%.

#### 4.4. Synthesis of compound (**1**)

To a methanol solution (10 mL) of  $Cu(ClO_4)_2 \cdot 6H_2O$  (0.134 g, 1 mmol), HL (1 mmol) in 15 mL of methanol was added with constant stirring. The resulting green solution was kept in boiling for 10 mins. After that in warm condition the mixture was kept undisturbed at room temperature. Dark-green rectangular-shaped single crystals of **1** were generated after one week. These were separated over filtration and air-dried before X-ray diffraction analysis. Yield: 0.73 g. Anal. Calc. for  $C_{19}H_{24}CuN_2O_6$ : C, 51.83; H, 5.51; N, 6.36. Found: C, 52.11; H, 5.28; N, 6.57%.

#### 4.5. X-ray crystallography

The crystal structure of **1** was determined by X-ray diffraction methods. Crystal data and experimental details for data collection and structure refinement are reported in **Table 3**. Intensity data and cell parameters were recorded at 100(2) K on a Bruker

Apex II (MoK $\alpha$  radiation,  $\lambda = 0.71073 \text{ \AA}$ ) equipped with a CCD area detector and a graphite monochromator. The  $\omega: 2\theta$  scan technique was applied within a  $\theta$  range of  $3.28\text{--}26.96^\circ$ . No significant crystal decay was observed. A total of 44565 reflections were collected of which 2114 were independent [ $R(\text{int}) = 0.0651$ ] reflections. The raw frame data were processed using Bruker SADABS to yield the reflection data file [60]. The structures were solved by Direct Methods using the SIR97 program [61] and refined on  $F_o^2$  by full-matrix least-squares procedures, using the SHELXL-2014/7 program [62] in the WinGX suite v.2014.1 [63,64]. All non-hydrogen atoms were refined with anisotropic atomic displacements. The weighting scheme used in the last cycle of refinement was  $w = 1/[\sigma^2 F_o^2 + (0.0379P)^2 + 2.5243P]$ , where  $P = (F_o^2 + 2F_c^2)/3$ . Geometric calculations were performed with the PARST97 program [65]. Crystallographic data (excluding structure factors) for the structure reported have been deposited with the Cambridge Crystallographic Data Centre as supplementary publication no. CCDC-1864043 for **1** and can be obtained free of charge on application to the CCDC, 12 Union Road, Cambridge, CB2IEZ, UK (fax: +44-1223-336-033; e-mail [deposit@ccdc.cam.ac.uk](mailto:deposit@ccdc.cam.ac.uk) or <http://www.ccdc.cam.ac.uk>).

**Table 3.** Crystallographic data of complex **1**.

Empirical formula	C <sub>19</sub> H <sub>24</sub> CuN <sub>2</sub> O <sub>6</sub>
Formula weight	439.94
Temperature	100(2)
Wavelength (Å)	0.71073
Crystal system	Orthorhombic
Space group	<i>Pnma</i>
<i>a</i> , Å	7.3675(2)
<i>b</i> , Å	21.9466(7)
<i>c</i> , Å	11.5763(4)
$\alpha$ , deg	90
$\beta$ , deg	90
$\gamma$ , deg	90
Volume, Å <sup>3</sup>	1871.79(10)
<i>Z</i>	4
D <sub>calc</sub> (mg m <sup>-3</sup> )	1.561
$\mu$ (Mo K $\alpha$ ) (mm <sup>-1</sup> )	1.207
F(000)	916
$\theta$ range for data collection	3.28 to 26.96
Total reflections	44565
Unique reflections ( <i>R</i> <sub>int</sub> )	2114 (0.0651)
Observed reflections [ <i>F</i> <sub>o</sub> > 4 $\sigma$ ( <i>F</i> <sub>o</sub> )]	1826
Data / restraints / parameters	2114 / 0 / 142
Final <i>R</i> indices [ <i>F</i> <sub>o</sub> > 4 $\sigma$ ( <i>F</i> <sub>o</sub> )] <sup>a</sup>	<i>R</i> 1 = 0.0318, <i>wR</i> 2 = 0.0868
Largest diff. Peak and	1.491 and -0.545

hole, $e.\text{\AA}^3$
------------------------

$${}^aR_1 = \frac{\sum |F_o| - |F_c|}{\sum |F_o|}, \quad wR_2 = \left[ \frac{\sum [w(F_o^2 - F_c^2)^2]}{\sum [w(F_o^2)^2]} \right]^{1/2}.$$

#### 4.6. Theoretical methods

The calculation of the EPR g-tensor has been performed using Gaussian-09 program [66] and the B3LYP/def2-TZVP level of theory. We have used the crystallographic coordinates for the calculation in the solid state where the positions of the H atoms have been optimized. For the calculation in solution, the geometry of the mononuclear complex has been fully optimized.

## Reference

- [1] K. Bowman-James, A. Bianchi, E. García-Espana, Wiley-VCH Verlag GmbH & Co., Weinheim, 2011.
- [2] K. Bowman-James, A. Bianchi, E. García-Espana, Wiley-VCH, New York, 1997.
- [3] V.K. Peterson, Y. Liu, C.M. Brown, C.J. Kepert, *J. Am. Chem. Soc.* 128 (2006) 15578-15579.
- [4] J.K. Clegg, S.S. Iremonger, M.J. Hayter, P.D. Southon, R.B. MacQuart, M.B. Duriska, P. Jensen, P. Turner, K.A. Jolliffe, C.J. Kepert, G.V. Meehan, L.F. Lindoy, *Angew. Chem., Int. Ed.* 49 (2010) 1075-1078.
- [5] L. Ma, C. Abney, W. Lin, *Chem. Soc. Rev.* 38 (2009) 1248-1256.
- [6] M.M. Wanderley, C. Wang, C.-D. Wu, W. Lin, *J. Am. Chem. Soc.* 134 (2012) 9050-9053.
- [7] J.M. Lehn, *Supramolecular Chemistry: Concepts and Perspectives*, Wiley-VCH, Weinheim, 1995.
- [8] W. Meng, B. Breiner, K. Rissanen, J.D. Thoburn, J.K. Clegg, J.R. Nitschke, *Angew. Chem., Int. Ed.* 50 (2011) 3479-3483.
- [9] W.J. Ramsay, T.K. Ronson, J.K. Clegg, J.R. Nitschke, *Angew. Chem., Int. Ed.* 52 (2013) 13439-13443.
- [10] L. Sacconi, I. Bertisi, R. Morassi, *Inorg. Chem.* 6 (1967) 1548-1553.

- [11] W.N. Wallis, S.C. Cummings, *Inorg. Chem.* 13 (1975) 986-991.
- [12] P. Bhattacharya, J. Parr, A.T. Ross, A.M.Z. Slawin, *J. Chem. Soc., Dalton Trans.* (1998) 3149-3150.
- [13] S. Basak, S. Sen, S. Banerjee, S. Mitra, G. Rosair, M.T.G. Rodriguez, *Polyhedron* 26 (2007) 5104-5112.
- [14] S. Mukherjee, P.S. Mukherjee, *Cryst. Growth Des.* 14 (2014) 4177-4186.
- [15] S. Kundu, S. Roy, K. Bhar, R. Ghosh, C.-H. Lin, J. Ribas, B.K. Ghosh, *J. Mol. Struct.* 1038 (2013) 78-85.
- [16] M.J. Zaworotko, *Cryst. Growth Des.* 7 (2007) 4-9.
- [17] G.A. Hembury, V.V. Borovkov, Y. Inoue, *Chem. Rev.* 108 (2008) 1-73.
- [18] Q. Ye, D.-W. Fu, H. Tian, R.-G. Xiong, P.W.H. Chen, S.D. Huang, *Inorg. Chem.* 47 (2008) 772-774.
- [19] X.-H. Chen, Q.-J. Wu, Z.-Y. Liang, C.-R. Zhan, J.-B. Liu, *Acta Crystallogr. Sect. C* 65 (2009) m190-m194.
- [20] V. Balzani, A. Credi, M. Venturi, *Molecular Devices and Machines*, vol. 4, Wiley-VCH, Weinheim, 2003.
- [21] J.S. Miller, in: M. Drillon (Ed.), *Magnetism: Molecules to Materials V*, vol. 5, Wiley-VCH, Weinheim, 2005, pp. 283-346.

- [22] J.-N. Liu, B.-W. Wu, B. Zhang, Y. Liu, Turk. J. Chem. 30 (2006) 41-47.
- [23] R.J. Butcher, E. Sinn, Inorg. Chem. 15 (1976) 1604-1608.
- [24] D. Reinen, C. Friebel, Inorg. Chem. 23 (1984) 791-798.
- [25] T. Ziegler, Pure App. Chem. 63 (1991) 873-878.
- [26] P. M. W. Gill, B. G. Johnson, J. A. Pople, M. J. Frisch, Chem. Phys. Lett. 197 (1992) 499-505.
- [27] A. Datta, K. Das, S.B. Mane, S. Mendiratta, M.S. El Fallah, E. Garribba, A. Bauza, A. Frontera, C.-H. Hung, C. Sinha, RSC Adv. 6 (2016) 54856-54865.
- [28] K. Das, U. Panda, A. Datta, S. Roy, S. Mondal, C. Massera, T. Askun, P. Celikboyun, E. Garribba, C. Sinha, K. Anand, T. Akitsu, K. Kobayashi, New J. Chem. 39 (2015) 7309-7321.
- [29] K. Das, A. Datta, S. Nandi, S.B. Mane, S. Mondal, C. Massera, C. Sinha, C.-H. Hung, T. Askun, P. Celikboyun, Z. Cantürk, E. Garribba, T. Akitsu, Inorg. Chem. Frontier 2 (2015) 749-762.
- [30] S. Thakurta, J. Chakraborty, G. Rosair, R.J. Butcher, S. Mitra, Inorg. Chim. Acta 362 (2009) 2828-2836.
- [31] K. Nakamoto, Infrared and Raman Spectra of Inorganic and Coordination Compounds, Theory and Applications in Inorganic Chemistry, 5th ed., John Wiley and Sons Inc., New York, 1997.

- [32] S.H. Rahaman, R. Ghosh, T.H. Lu, B.K. Ghosh, *Polyhedron* 24 (2005) 1525-1532.
- [33] M. Dolaz, M. Tümer, M. Digrak, *Trans. Met. Chem.* 29 (2004) 528-538.
- [34] Z.L. You, H.L. Zhu, *Z. Anorg. Allg. Chem.* 630 (2004) 2754-2760.
- [35] A. Golcu, M. Tümer, H. Demirelli, R.A. Wheatley, *Inorg. Chim. Acta* 358 (2005) 1785-1797.
- [36] M. Dieng, I. Thiam, M. Gaye, A.S. Sall, A.H. Barry, *Acta Chim. Slov.* 53 (2006) 417-423.
- [37] H. Adams, N.A. Bailey, I.S. Bard, D.E. Fenton, J.-P. Costes, G. Cros, J.P. Laurent, *Inorg. Chim. Acta* 101 (1985) 7-12.
- [38] E. Kwiatkowski, M. Kwiatkowski, *Inorg. Chim. Acta* 117 (1986) 145-149.
- [39] M. Kwiatkowski, G. Bandoli, *J. Chem. Soc., Dalton Trans.* (1992) 372-377.
- [40] M.S. Hussain, E.O. Schlemper, *Inorg. Chem.* 18 (1979) 2275-2282.
- [41] A.C. Rizzi, N. I. Neuman, P.J. González, C.D. Brondino, *Eur. J. Inorg. Chem.* (2016) 192-207.
- [42] B.J. Hathaway, D.E. Billing, *Coord. Chem. Rev.* 5 (1970) 143-207.
- [43] B.J. Hathaway, *Struct. Bond.* 57 (1984) 55-118.
- [44] E. Garribba, G. Micera, *J. Chem. Ed.* 83 (2006) 1229-1232.
- [45] S. Thakurta, C. Rizzoli, R.J. Butcher, C.J. Gomez-Garcia, E. Garribba, S. Mitra,

Inorg. Chim. Acta 363 (2010) 1395-1403.

[46] A. Ray, S. Mitra, A.D. Khalaji, C. Atmani, N. Cosquer, S. Triki, J.M.

Clemente-Juan, S. Cardona-Serra, C.J. Gomez-Garcia, R.J. Butcher, E.

Garribba, D. Xu, Inorg. Chim. Acta 363 (2010) 3580-3588;

[47] A. Datta, J.K. Clegg, J.-H. Huang, A. Pevec, E. Garribba, M. Fondo, Inorg.

Chem. Comm. 24 (2012) 216-220.

[48] K. Das, A. Datta, S. Roy, J.K. Clegg, E. Garribba, C. Sinha, H. Kara,

Polyhedron 78 (2014) 62-71;

[49] S. Saha, A. Sasmal, C.R. Choudhury, C.J. Gomez-Garcia, E. Garribba, S. Mitra,

Polyhedron 69 (2014) 262-269;

[50] A. Datta, K. Das, C. Massera, J.K. Clegg, C. Sinha, J.-H. Huang, E. Garribba,

Dalton Trans. 43 (2014) 5558-5563.

[51] M.M. Bhadbhade, D. Srinivas, Inorg. Chem. 32 (1993) 5458-5466.

[52] M. Valko, R. Boca, R. Klement, J. Kožíšek, M. Mazúr, P. Pelikán, H. Morris,

H. Elias, L. Müller, Polyhedron 16 (1997) 903-908.

[53] E.H. Charles, L.M.L. Chia, J. Rothery, E.L. Watson, E.J.L. McInnes, R.D.

Farley, A.J. Bridgeman, F.E. Mabbs, C.C. Rowlands, M.A. Halcrow, J. Chem.

Soc., Dalton Trans. (1999) 2087-2095.

[54] R. Klement, F. Stock, H. Elias, H. Paulus, P. Pelikán, M. Valko, M. Mazúr,

Polyhedron 18 (1999) 3617-3628.

[55] S. Thakurta, J. Chakraborty, G. Rosair, J. Tercero, M.S. El Fallah, E. Garribba,

S. Mitra, Inorg. Chem. 47 (2008) 6227-6235.

[56] O. Kahn, Molecular Magnetism, VCH, New York, 1993.

[57] C. Jayakumar, C.M. Magdalane, K. Kaviyarasu, M.A. Kulandainathan, B.

Jeyaraj, M. Maaza, J. Nanosci. Nanotechnol. 18, (2018) 1-7.

[58] K. Fricke, F. Harnisch, U. Schroder, Energy Environ. Sci. 1 (2008) 144-147.

[59] *WINEPR SimFonia, version 1.25*, Bruker Analytische Messtechnik GmbH,

Karlsruhe, 1996.

[60] SADABS Bruker AXS; Madison, Wisconsin, USA, 2004; SAINT, Software

Users Guide, Version 6.0; Bruker Analytical X-ray Systems, Madison, WI

(1999). G. M. Sheldrick, SADABS v2.03: Area-Detector Absorption Correction.

University of Göttingen, Germany (1999).

[61] A. Altomare, J. Appl. Cryst. 32 (1999) 115-119.

[62] G.M. Sheldrick, Acta Crystallogr. A64 (2008) 112-122.

[63] L.J. Farrugia, J. Appl. Crystallogr. 45 (2012) 849-854.

[64] P. v.d. Sluis, A.L. Spek, Acta Cryst. Sect A. 46 (1990) 194-201.

[65] M. Nardelli, J. Appl. Crystallogr. 29 (1996) 296-300.

[66] M.J. Frisch, G.W. Trucks, H.B. Schlegel, G.E. Scuseria, M.A. Robb, J.R.

Cheeseman, G. Scalmani, V. Barone, B. Mennucci, G.A. Petersson, H. Nakatsuji,  
M. Caricato, X. Li, H.P. Hratchian, A.F. Izmaylov, J. Bloino, G. Zheng, J.L.  
Sonnenberg, M. Hada, M. Ehara, K. Toyota, R. Fukuda, J. Hasegawa, M. Ishida,  
T. Nakajima, Y. Honda, O. Kitao, H. Nakai, T. Vreven, J.A. Montgomery Jr, J.E.  
Peralta, F. Ogliaro, M. Bearpark, J.J. Heyd, E. Brothers, K.N. Kudin, V.N.  
Staroverov, R. Kobayashi, J. Normand, K. Raghavachari, A. Rendell, J.C. Burant,  
S.S. Iyengar, J. Tomasi, M. Cossi, N. Rega, M.J. Millam, M. Klene, J.E. Knox,  
J.B. Cross, V. Bakken, C. Adamo, J. Jaramillo, R. Gomperts, R.E. Stratmann, O.  
Yazyev, A.J. Austin, R. Cammi, C. Pomelli, J.W. Ochterski, R.L. Martin, K.  
Morokuma, V.G. Zakrzewski, G.A. Voth, P. Salvador, J.J. Dannenberg, S.  
Dapprich, A.D. Daniels, Ö. Farkas, J.B. Foresman, J.V. Ortiz, J. Cioslowski, D.J.  
Fox, Gaussian, Inc, Wallingford CT, 2009.

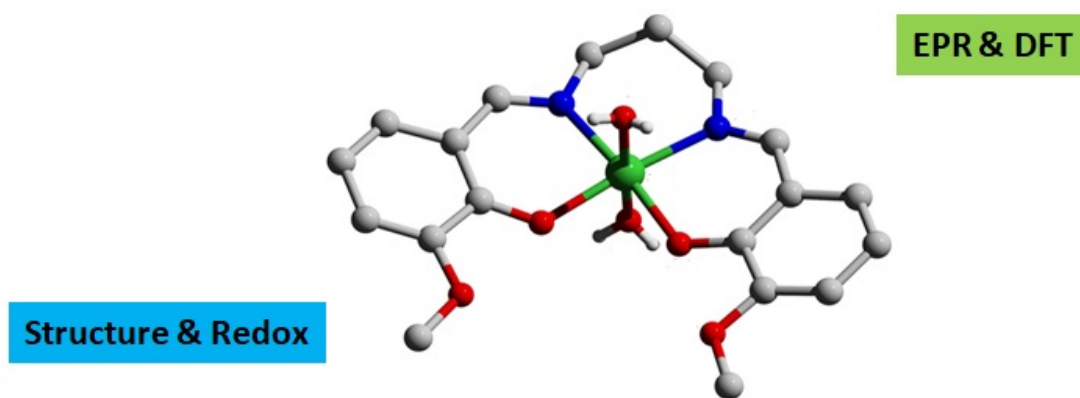
### **Pictogram for Graphical Abstract**

**EPR, DFT and Electrochemical Interpretation of a Cu(II) Derivative**

**Incorporating a Schiff Base Precursor**

Kuheli Das,<sup>\*a</sup> Sanchita Goswami,<sup>a</sup> Belete B. Beyene,<sup>b,d</sup> Amogne W. Yibeltal,<sup>b,c</sup>

Eugenio Garribba,<sup>e</sup> Antonio Frontera,<sup>f</sup> Amitabha Datta,<sup>\*b</sup>



### Synopsis for Graphical Abstract

#### **EPR, DFT and Electrochemical Interpretation of a Cu(II) Derivative Incorporating a Schiff Base Precursor**

Kuheli Das,<sup>\*a</sup> Sanchita Goswami,<sup>a</sup> Belete B. Beyene,<sup>b,d</sup> Amogne W. Yibeltal,<sup>b,c</sup>

Eugenio Garribba,<sup>c</sup> Antonio Frontera,<sup>f</sup> Amitabha Datta,<sup>\*b</sup>

A new mononuclear Cu(II) derivative is afforded incorporating the potentially di-compartmental hexadentate Schiff base precursor. Besides the X-ray structure, DFT computation is subjected to evident the geometrical and spectral nature of the complex. Additionally, the electrochemical study confirms the presence of three reversible redox potentials among the Cu(II) system.

---

**Table 1.** Selected bond lengths (Å) and angles (°) of compound **1**.

Cu1-N1	2.073(2)	Cu1-O1	2.015(2)	Cu1-O3	2.089(2)
Cu1-O4	2.103(2)	N1-C1	1.286(3)	N1-Cu1-N1'	97.10(7)
O1-Cu1-O3	91.37(8)	O1-Cu1-O4	91.99(8)	O1-Cu1-N1	88.43(6)
O1-Cu1-O1'	86.03(6)	O3-Cu1-O4	175.40(9)	O1'-Cu1-N1	174.45(7)

---